

Multi-input interleaved DC-DC converter for hybrid renewable energy applications

Ibrahim Alhamrouni¹, Mohamed Salem², Younes Zahraoui¹, Bazilah Ismail¹, Awang Jusoh³, Tole Sutikno⁴

¹Electrical Engineering Section, University Kuala Lumpur (UniKL BMI), Kuala Lumpur, Malaysia

²School of Electrical and Electronic Engineering, Universiti Sains Malaysia, Penang, Malaysia

³School of Electrical Engineering, Universiti Teknologi Malaysia, Johor, Malaysia

⁴Department of Electrical Engineering, Universitas Ahmad Dahlan, Yogyakarta, Indonesia

Article Info

Article history:

Received Aug 5, 2021

Revised Apr 20, 2022

Accepted May 25, 2022

Keywords:

DC-DC boost converter
Hybrid renewable energy
Interleaved converter
Multi-input converter

ABSTRACT

The increasing demand for hybrid energy systems based on renewable energy sources has enabled the new dimension for multi-input converter (MIC). Various topologies have been introduced over the last decade. However, most of these topologies have several drawbacks in terms of design complexity or efficiency. Therefore, this research aims to introduce a multi-input DC-DC converter for hybrid renewable energy applications. The proposed multi-input converter is able to hybridize different sources such as solar PV array and PEMFC. Analysis and simulation have been carried out for the double input two-phase interleaved converter in operating the boost mode. The proposed converter is designed in matlab simulink by using interleaved boost converter method to achieve a boosted and smoothened output. The proposed topology has shown a remarkable performance in terms of output voltage boosting, voltage ripple reduction as well as enhanced efficiency through interleaved boosting technique. From the simulation results, it can be observed that the proposed converter can gain high efficiency which is higher than 97%. The obtained results have been validated with previously published works and the proposed technique has been proven to yield compatible and improved outcomes.

This is an open access article under the [CC BY-SA](https://creativecommons.org/licenses/by-sa/4.0/) license.



Corresponding Author:

Ibrahim Alhamrouni

Electrical Engineering Section, University Kuala Lumpur British Malaysian Institute (UniKL BMI)

Kuala Lumpur, Malaysia

Email: ibrahim.mohamed@unikl.edu.my

1. INTRODUCTION

In recent years, the demand for renewable energy shows an inclined interest where the reliance on variable renewable energy sources continued to rise as the energy has been established globally [1], [2]. In 2018, at least one gigawatt of generating capacity had been installed in more than 90 countries, while more than thirty countries reached a 10GW capacity. In some areas, wind and solar photovoltaic power have been further expanded their percentages and the increasing number of countries now have variable renewables in the energy mixes more than 20% [3], [4]. The rising price for fossil fuels and worries about the environmental impacts of greenhouse gas emissions have renewed interest in alternative energy supply production [5], [6]. Renewable energy is considered a more sustainable carbon option and a better alternative compared to conventional sources of energy [7], [8].

However, the intermittency of renewable energy produced less efficient energy than non-renewable energy due to weather dependency [9], [10]. A hybrid renewable energy system, which is gaining popularity in the field as electrical systems are considered by researchers to be an emerging technology with the

potential to meet future energy needs that increase significantly each year [11], [12]. Several researchers have considered the hybrid system mode of renewable energy to address the intermittent and volatility of renewable sources and provide a stable supply of electricity. A hybrid combination of two or more renewable energy sources and their integration make the best use of their operational characteristic and increase both system performance and efficiency [13], [14].

A hybrid renewable energy power system seems to be the long-term power solution for electrical power system applications. This has led to plenty of studies that focus on the hybrid power system. One of the focuses is the power electronic converter that is used in hybrid systems, whereas most of the hybrid systems are complex and expensive due to numerous uses of power converters [15], [16]. Another issue that has been encountered, which is the low efficiency of the converters and the high cost to design a converter that is able to boost and smoothen the output voltage to suit the power system requirement [17], [18]. This work aims to design a multi-input boost DC-DC converter for hybrid renewable energy applications. Furthermore, the designed DC-DC converter boosting applicability and compatibility will be tested.

There have been many proposed topologies to boost the voltage with higher efficiency. Among the important studies are the following: the works presented [19], [20] proposed the dual input dc-dc converter by using fuzzy logic control. The main function of the fuzzy logic control scheme is to jumble a different non-linear characteristic source which is used to tune PID controller parameters and adjust the duty ratios of dual input dc-dc converter. Another important work introduced [21], the work proposes two input interleaved boost converters connected to a cascading structure and is synthesized using pulsating current source cell (PCSC). Furthermore, the work in [22] proposes a multi-input single-phase interleaved boost converter for hybrid renewable energy. The method proposed an interleaved technique with two step-up converters and two-hybrid inputs are accommodating with extra semiconductors, diodes, and inductances.

Development of the previous works continued with another work presented [23], this work proposes to use a combination of the boost converter and a quasi Y-source dc-dc converter in the double input converter. Besides, work done by [24] has proposed the use of isolated 3-port dc-dc converter focused on interleaved boost full-bridge converter with PWM and phase shift control [25]. The previous published works suffer some important drawbacks in many aspects that limit their application [26], [27]. Table 1 shows the drawbacks of previous studies summary.

Table 1. Drawbacks of previous studies

Topology of converter	Efficiency	Cost	Control method	Design complexity	Effectiveness
Dual input DC-DC converter using fuzzy logic control	Moderate	High	Fuzzy logic control for duty cycles	Simple	Moderate
Pulsating current sources cell (PCSC) interleaved boost converter	High	High	Pulsating current sources cell	Complex	High
Multi-input single phase interleaved boost converter	Low	Low	Single interleaved converter	Simple	Low
Double input boost/Y-source DC-DC converter	High	High	Boost & Y source converter	Complex	High
Dual input interleaved boost full bridge three-port converter	High	High	Three port converter	Complex	Low

This paper is organized as: section 2 presents the circuit topology, operation of the multi-input interleaved boost converter, and distributed generation sources. Whereas section 3 deals with the simulation of the converter and analysis of the obtained results. Finally, the conclusion and future work is discussed in section 4.

2. RESEARCH METHODOLOGY

This section will present a novel proposed technique to cover the drawbacks experienced by the previously designed ones. The proposed technique is based on two phases interleaved multi-input DC-DC boost converter for the application of renewable energy. The proposed topology is expected to perform superiorly with respect to the techniques available in the literature, this section introduces a multiple-input DC-DC interleaved boost converter. The newly proposed converter will be discussed in detail from the aspect of design, applications, and operation modes and their transfer function.

2.1. Proposed multi-input DC-DC converter

The proposed multi-input converter is basically a two-phase interleaved technique boosting converter for two-hybrid DC inputs which are solar PV array and PEMFC. The converter is operating in six operation modes [28], [29]. The operating principle of the converter is the same as the conventional converter, which charges the first inductor from the source and then transfers the energy to the load. Both

inductors are operating in complementary mode. While one of the inductors is charged, another inductor is discharged to the load and vice versa. Since the converter only operates in boost mode, by depending on the switching technique, either one or both sources must be connected to the inductor all the time, as shown in Figure 1.

The intermediate switching technique is utilized to acquire the modulated power supply at the pole-point of the converter, which voltage at this point is known as V_p . The switching technique proposed in the converter for the bulk cell switches (S_1 & S_2) are high frequency and high current switches which are MOSFETs, while T_1 and T_2 are high-frequency transistors with half the current rate which are IGBTs. Considering Dx and Dy assigned duty cycle for transistors T_1 and T_2 to perform interleaving operation. The duty cycles for each switch is given in (1) to (4) [17].

$$D1 = \frac{(t1+t2+t5+t6)}{T_s} \quad (1)$$

$$D2 = \frac{(t2+t3+t4+t5)}{T_s} \quad (2)$$

$$Dx = \frac{(t1+t2+t3)}{T_s} \quad (3)$$

$$Dy = \frac{(t4+t5+t6)}{T_s} \quad (4)$$

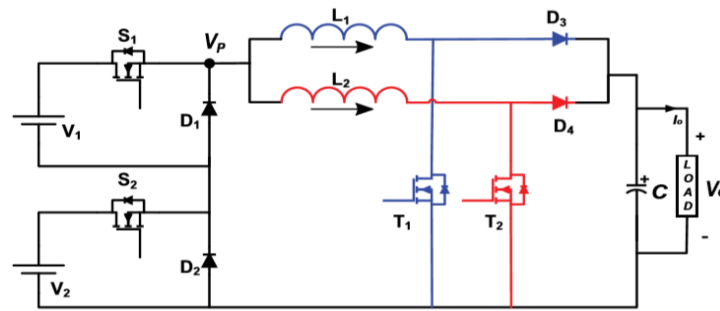


Figure 1. Proposed multi input DC-DC boost converter

Mode 1: $[0 < t < t_1]$, V_1 is energizing L_1 while $V_1 - V_0$ is discharging L_2 . S_1 is conducted while S_2 remains non-conducting. D_1 is reverse biased while the T_1 and T_2 are conducting in complementary mode. The equivalent circuit of this mode is shown in Figure 2(a). The sources V_1 will charge the inductors and the voltage across the two inductors are as (5) and (6).

$$L \frac{\delta i_{L1}}{\delta t} = V_1 \quad (5)$$

$$L \frac{\delta i_{L2}}{\delta t} = V_0 - V_2 \quad (6)$$

Mode 2: $[t_1 < t < t_2]$, V_1 and V_2 conduct the inductor L_1 in series and charge during this time, meanwhile energy stored in L_2 is transferred to the load. Equations related to this mode are in (7) and (8). The equivalent circuit of this mode is shown in Figure 2(b).

$$L \frac{\delta i_{L1}}{\delta t} = V_1 + V_2 \quad (7)$$

$$L \frac{\delta i_{L1}}{\delta t} = V_0 - (V_1 + V_2) \quad (8)$$

Mode 3: $[t_2 < t < t_3]$, switch S_1 will be disconnected, the system will then be governed by a single source V_2 . This source will provide the energy to the load and L_1 . This mode is given in Figure 2(c) which also holds the charging and discharging slopes given by (9) and (10).

$$L \frac{di_{L1}}{dt} = V_2 \quad (9)$$

$$L \frac{di_{L1}}{dt} = V_0 - V_1 \quad (10)$$

Mode 4: $[t_3 < t < t_4]$, switch T_1 and T_2 get reversed. The presents of V_2 cause the inductor L_2 begins to energize and with the level of output voltage, L_1 supplies the stored energy to the load. At this time, D_2 and D_4 will act as reversed biased, meanwhile, D_1 and D_3 are conducting mode. Equation related to this mode is as (11) and (12) whereas the equivalent circuit is presented in Figure 2(d).

$$L \frac{di_{L1}}{dt} = V_0 - V_1 \quad (11)$$

$$L \frac{di_{L1}}{dt} = V_2 \quad (12)$$

Mode 5: $[t_4 < t < t_5]$, inductor L_2 is charged by V_1 and V_2 in series, while L_1 is starting to discharge to the load. Related equations are present in (13) and (14) and the equivalent circuit is shown in Figure 2(e).

$$L \frac{di_{L1}}{dt} = V_0 - (V_1 - V_2) \quad (13)$$

$$L \frac{di_{L1}}{dt} = V_1 + V_2 \quad (14)$$

Mode 6: $[t_5 < t < t_6]$, S_2 is OFF while S_1 is ON which resulting the diode D_2 in forward biased condition. In (15) and (16) represents the status in this mode. The equivalent circuit is shown in Figure 2(f).

$$L \frac{\delta i_{L1}}{dt} = V_0 - V_1 \quad (15)$$

$$L \frac{\delta i_{L1}}{dt} = V_1 \quad (16)$$

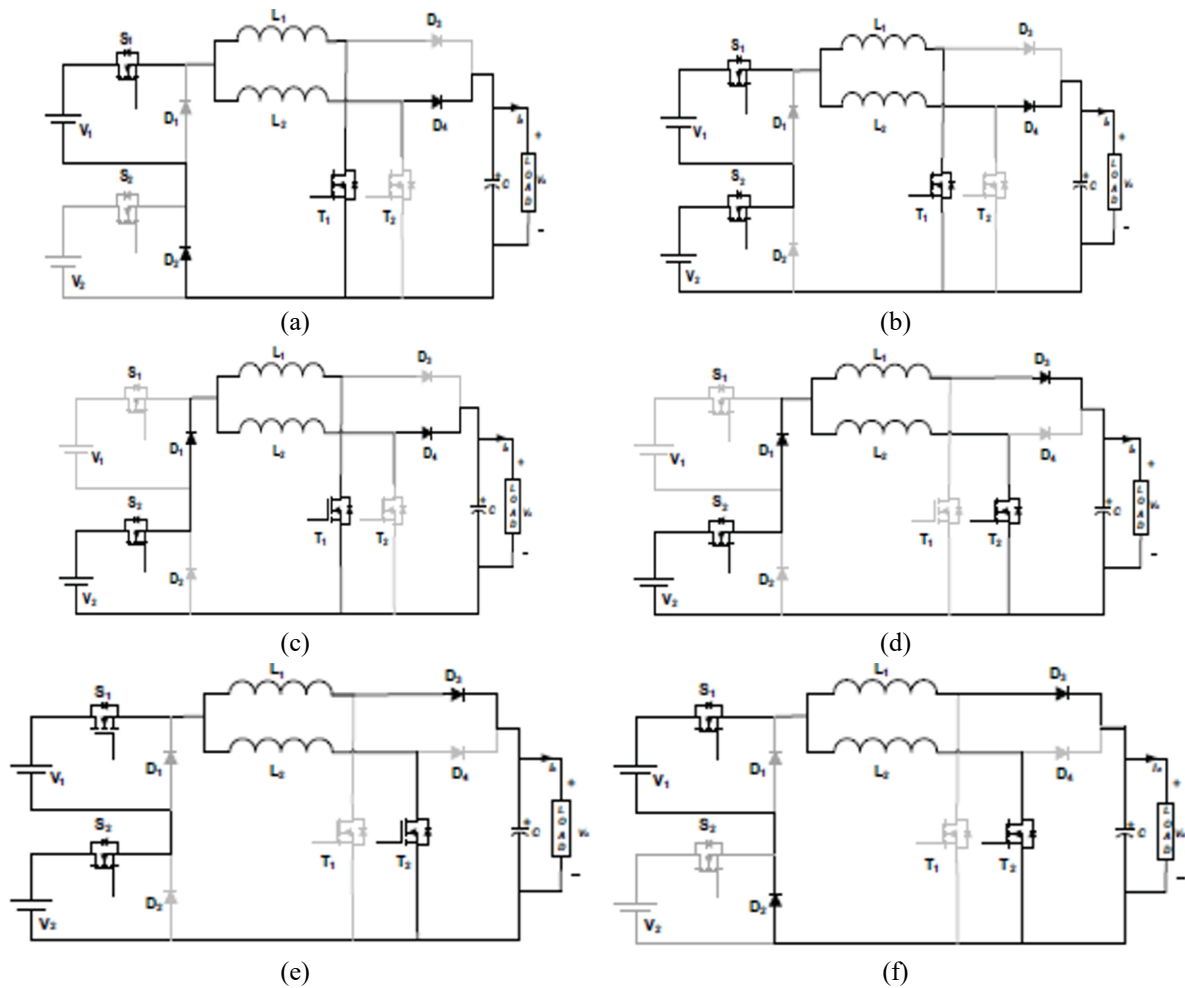


Figure 2. Operation modes of dual input interleaved boost converter (a) mode-1 for $0 < t < t_1$, (b) mode-2 for $t_1 < t < t_2$, (c) mode 3 for $t_2 < t < t_3$, (d) mode-4 $t_3 < t < t_4$, (e) mode-4 for $t_3 < t < t_4$, (e) $t_4 < t < t_5$ and (f) mode-6 $t_5 < t < t_6$

2.2. Design parameters of interleaved boost converter

The proposed interleaved boost converter consists of two phases that operate in 180° phase delay. The converter is aimed to produce a single fixed DC output voltage where the inputs are from two sources [30], [31]. To regulate the output of the converter, a closed-loop control is used. The block diagram of closed-loop converter is shown in Figure 3.

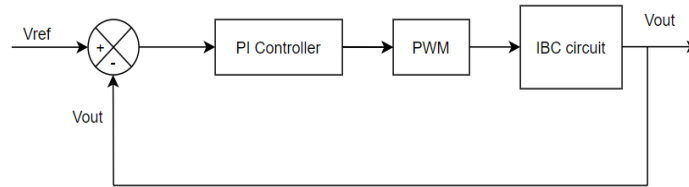


Figure 3. Block diagram of closed-loop interleaved boost converter

The converter is considered to operate in continuous conduction mode (CCM) in steady-state conditions. Proper selection of inductors, capacitors, and power semiconductor devices are required to reduce the switching losses in the converter [32], [33]. The step to design an interleaved converter are as: i) selection of duty cycles; ii) selection of load resistance; iii) selection of power semiconductor switches; iv) design of inductance and capacitance.

The two phases interleaved boost converter is derived based on the formulas of a single input boost converter in a steady state. The steady-state characteristics of the interleaved converter are as shown in (17) to (23).

a. Selection of duty cycles

The number of interleaved phases chosen for this study is two, where the ripples in the input current and output voltage decrease with the increasing number of interleaved phases. The duty cycles of switches T_1 and T_2 are decided based on the number of phases, where the least ripples can be adjusted by a certain duty ratio [20]. For two phases of interleaved converter, the ripple is the least at a duty cycle of 0.45 to 0.5. therefore, the design value of the duty cycle is chosen as 0.5.

b. Selection of load resistance

The output voltage formula for two phases interleaved boost converter differs from the conventional boost converter where the formula must consider both input voltages from both sources. The output voltage, V_o is given by (17).

$$V_o = \frac{(V_1 D_1) + (V_2 D_2)}{D_y} = \frac{(V_1 D_1) + (V_2 D_2)}{1 - D_x} \quad (17)$$

The output current of the converter can be calculated by the output power and output voltage. The output current is given by (18).

$$I_o = \frac{P_o}{V_o} \quad (18)$$

From the output voltage and output current, the value of load resistance can be calculated based on in (19).

$$R = \frac{V_o}{I_o} \quad (19)$$

c. Selection of power semiconductor switches

The semiconductor devices chosen to construct the dual input two phases interleaved converter are metal oxide semiconductor field effect transistor (MOSFET) and insulated gate bipolar transistor (IGBT). MOSFET is used as the switches SW_1 and SW_2 while IGBT is chosen for switches T_1 and T_2 . MOSFET provides benefits where the absence of gate current results in high input impedance producing high switching speed. Besides, MOSFET also provides greater efficiency while operating at lower voltages. The characteristic of MOSFET makes it best suited to be chosen for SW_1 and SW_2 where these switches require a high frequency high current switch [34], [35].

Even though MOSFET is a high switching device, IGBT is chosen for switches T_1 and T_2 . IGBT usage is predominated for higher voltage applications as it is unipolar and requires additional freewheeling diode for the reverse flow of current. Because of this additional diode, IGBT provides very high performance compared to the MOSFET which is most suitable for switches T_1 and T_2 . selection of inductor and capacitor [36].

In the interleaved boost converter, the inductor is used to convert the energy from the input voltage to the inductor current and convert it back to the output voltage from the induction current. As per the

principle of the two inductors are identical to balance the current in the converter. The inductor 1, L_1 and inductor 2, L_2 are obtained based on the relationship in (20).

$$L \geq \frac{V_o}{k_{fsw} \Delta i_L} (1 - Dx) \quad (20)$$

The inductor current ripple peak to peak amplitude can be determined by (21) and the output capacitor, C_{out} is given by (22).

$$\Delta i_{L1, iL2} = \frac{(V_{1D1} + V_{2D2})}{f_{sw} L} (Dx) \quad (21)$$

$$C_{out} \geq \frac{V_o}{R_{fs} \Delta v_c} (Dx) = \frac{V_o}{R_{fs} \Delta v_c} (1 - Dy) \quad (22)$$

d. Considered parameter for input voltage

The efficiency of the converter is calculated based on (23) which is represented by the ratio of output and input power. Energy conversion efficiency, η is the ratio between the useful output of energy conversion and the input.

$$\eta = \frac{V_o \cdot I_o}{V_{in} \cdot I_{in}} \times 100\% \quad (23)$$

The ranges of input and output voltage of the multi-input interleaved boost converter is based on switches and transistors' duty cycles limit. The first input voltage limit is considered between 45V to 65V which is suitable with PEMFC application. Where the duty cycle for switch SW_1 is fixed to 0.8. the second input voltage is considered to supply within 20V to 90V, where the duty cycle of switch SW_2 can be arranged between 0.2 to 0.9 duty cycle.

2.3. Generation of renewable energy sources

The generation sources of the interleaved converter are based on two types of renewable energy which are photovoltaic solar energy and fuel cell, where both energies are dc sources. The equivalent circuit, related parameters, and formulas for solar and fuel cell is shown below.

– Proton exchange membrane fuel cell modelling

The proton exchange membrane fuel cell (PEMFC) was designed by using the available model block in the simulink library. Figure 4 shows the designed PEMFC in the MATLAB Simulink. The PEMFC has been designed based on the parameters discussed in the previous section. Table 2 shows the parameters of the PEMFC used in this work.

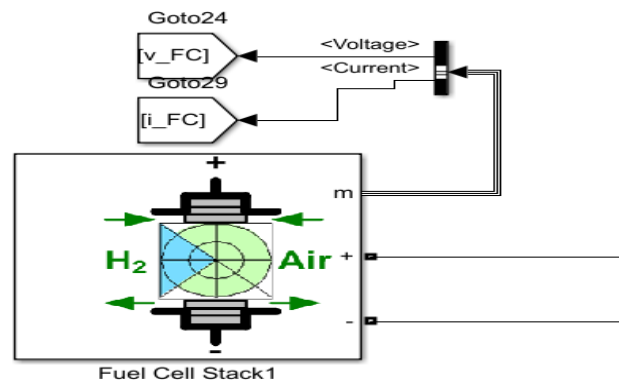


Figure 4. PEMFC model

– Solar photovoltaic modelling

A generalized PV array is constructed in MATLAB/Simulink which illustrates and verify the characteristic of PV module. The proposed model is carried out and is proven in Figure 5. Figure 6 demonstrates the subsystem implementation of the diode block and Figure 7 shows the designed PV array. A photovoltaic solar system has been designed by using matlab simulink. Table 3 shows the parameters of the PV array used as one of the DC voltage input of the interleaved converter.

Table 2. Parameters of PEMFC

Parameters	Value
Rated output power, P_o	6kW
Nominal current, I_{nom}	133.3A
Nominal voltage, V_{nom}	45V
Current at maximum power, I_m	225A
Voltage at maximum power, V_m	37V
Nominal stack efficiency, η_{nom}	55%
Number of cells, N	65
Operating temperature, T	65°C
Nominal supply pressure of [H ₂ , Air]	1.5, 1
Nominal composition percentage (%) [H ₂ , O ₂ , H ₂ O]	99.95, 21, 1

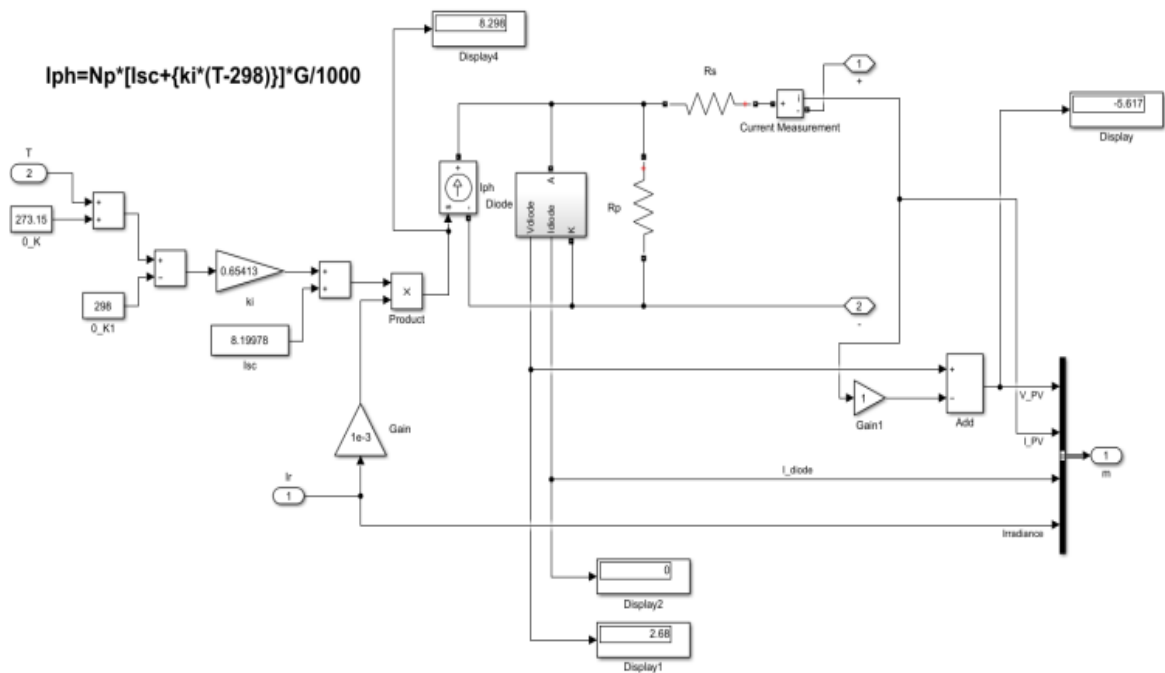


Figure 5. Subsystem of general PV array

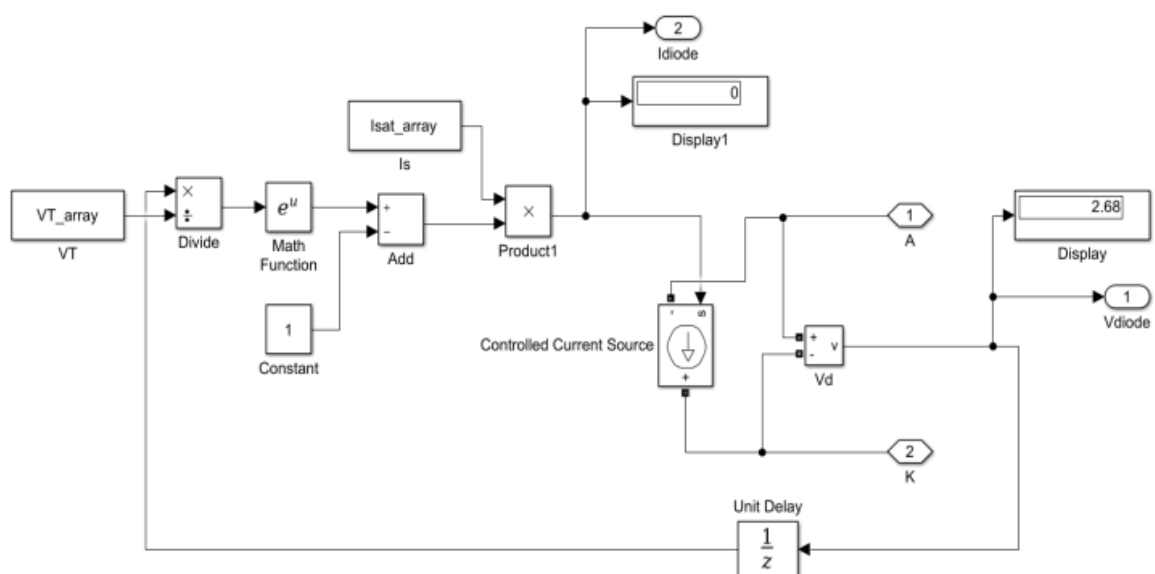


Figure 6. Subsystem of diode block

Table 3. Parameters of PV array

Parameters	Values
Number of solar cells per module	72
Number of series connected module per string, N_s	6
Number of parallel strings, N_p	3
Open circuit voltage, V_{oc}	45V
Short circuit current, I_{sc}	8.2 A
Voltage at maximum power, V_{mp}	35 V
Current at maximum power, I_{mp}	7.71 A
Rated power, P_{mp}	6kW
Series resistance, R_s	0.32025
Shunt resistance, R_{sh}	2562.3
Saturation current, I_{sat}	8.8992e-7
Photocurrent, I_{ph}	8.2979
Diode quality factor, n	1.5

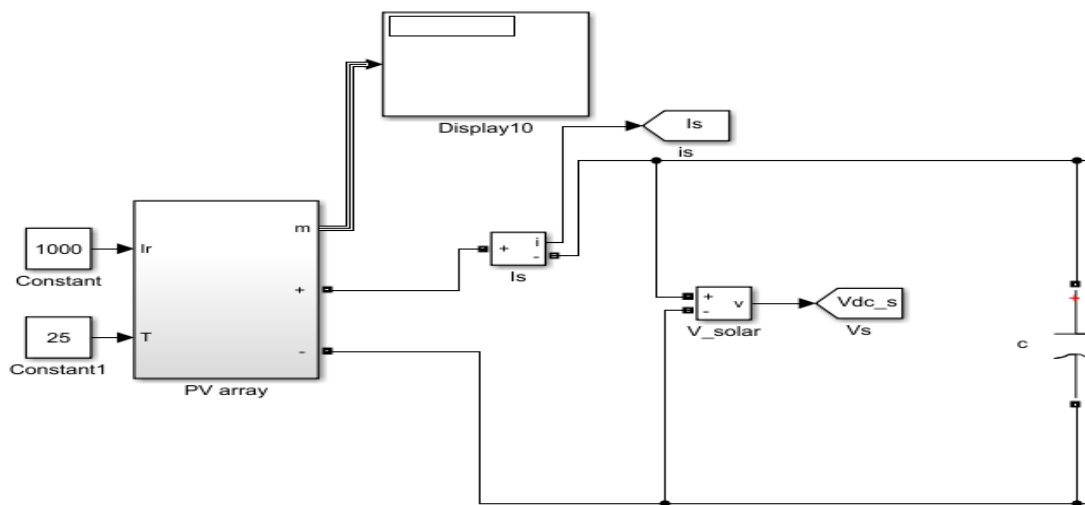


Figure 7. Designed PV array

3. RESULTS AND DISCUSSION

Simulation tests for multi-input interleaved boost converter have been performed. Results obtained and analyzed for CCM mode were conducted under consideration of a steady-state condition. The converter has been designed to be tested with renewable energy sources which are solar PV array and PEMFC. The converter has been tested with the parameters illustrated in Table 4, where the solar PV array varies with different irradiation values. The irradiation values are 500 W/m², 750 W/m² and 1000W/m² with 25°C of temperature. PEMFC in the converter acted as a control variable where the parameter used for each case are the same. The boosting ability and compatibility between the solar PV array and PEMFC have been tested. Table 5 shows the parameters used in the simulation of the converter with renewable energy sources.

Table 4. Parameters for multi-input interleaved converter simulation

Parameter	Value (unit)
Output voltage, V_{out}	140V
Output power, P_{out}	980W
Output current, I_{out}	7A
Switching frequency, f_{sw}	50kHz
Inductors, $L_1=L_2$	5mH
Current ripple, Δi_L	$\cong 20\%$
Capacitor, C	100 μ F

Input and inductor current for MIIBC with RE sources of Figure 8 case I, Figure 9 case II, Figure 10 case III, shows the input and inductor current comparison of multi-input interleaved boost converter with renewable energy sources for case I, case II, and case III. The input current and current through the inductor for each case are shown in Figures 8, 9, and 10. From the figures, it can be observed that the input current for the three cases are 14.325 A, 14.36 A, and 14.37 A, respectively. Meanwhile, the current through inductors

for each case is shown by the inductor current waveform in the Figures are 7.205 A, 7.22 A, and 7.22 A, individually. The input current ripples for each case can be obtained from the figures as 0.075 A, 0.13 A, and 0.15 A, respectively.

Table 5. Renewable energy input parameters

Case	PEMFC	Solar PV		
	Input voltage 1 (V)	Irradiance (W/m ²)	Temperature (°C)	Input voltage 2 (V)
I	65	500	25	41.71
II	65	750	25	62.21
III	65	1000	25	82.72

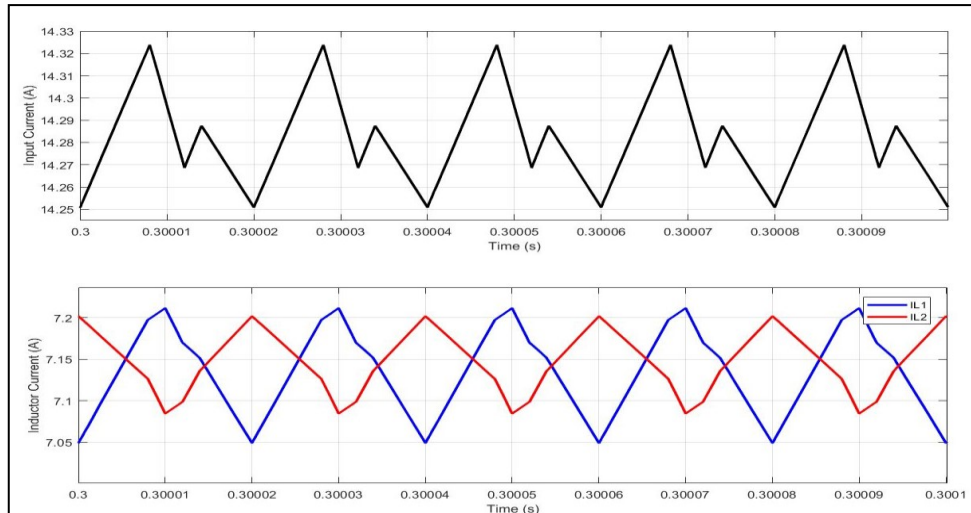


Figure 8. Input and inductor current for MIIBC with RE sources case I

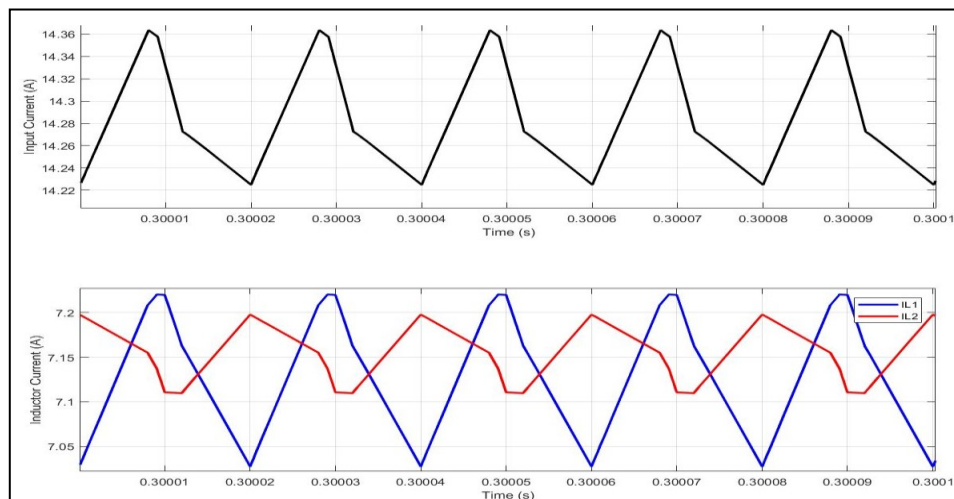


Figure 9. Input and inductor current for MIIBC with RE sources case II

Output voltage and current for MIIBC with RE sources of Figure 11 case I, Figure 12 case II, Figure 13 case III shows the comparison of the output voltage and output current of the multi-input interleaved boost converter with renewable energy sources for three cases. Figures 11, 12, and 13 show the output voltage and output current ripples for each case. The output voltage waveform in the figures shows that the ripples for each case are 2.5 mV, 4 mV, and 5 mV, respectively. Furthermore, the output current ripples for each case also can be observed from the figures which are 0.13 mA, 0.15 mA, and 0.2 mA, individually. From the output voltage waveforms, the times for each case to reach the desired output voltage are observed as 0.09s, 0.055s, and 0.045s, respectively.

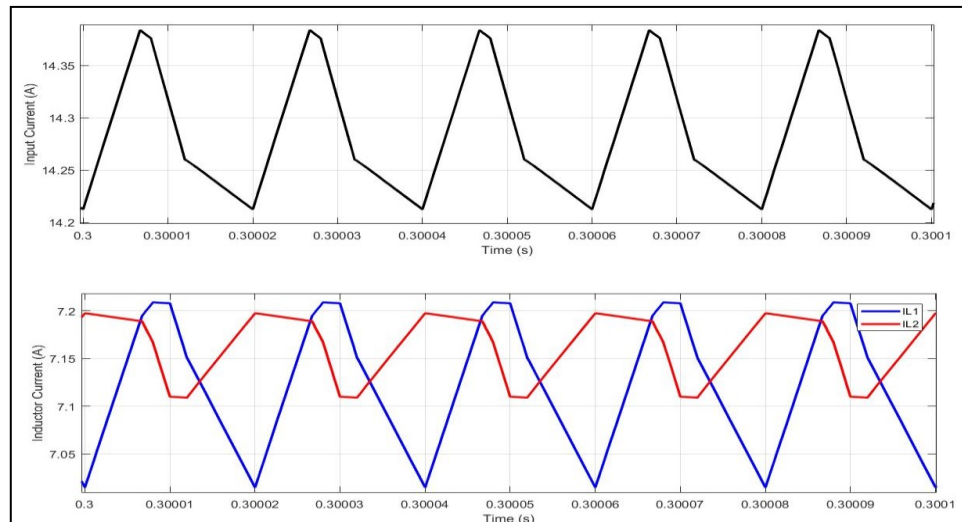


Figure 10. Input and inductor current for MIIBC with RE sources case III

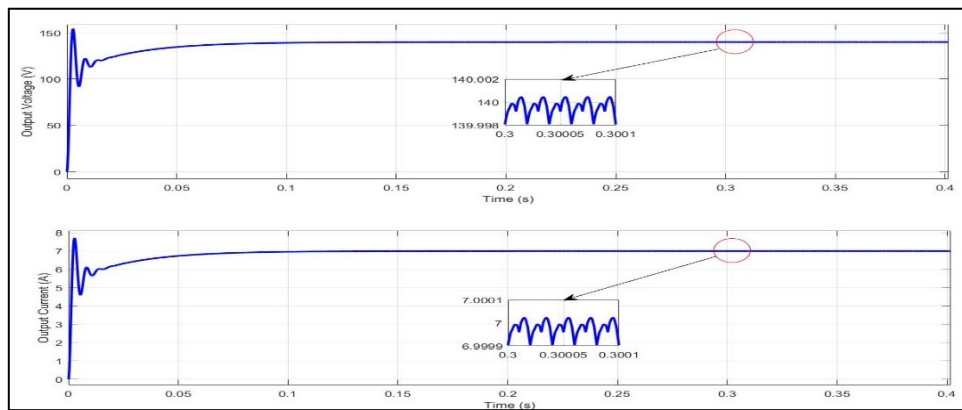


Figure 11. Output voltage and current for MIIBC with RE sources case I

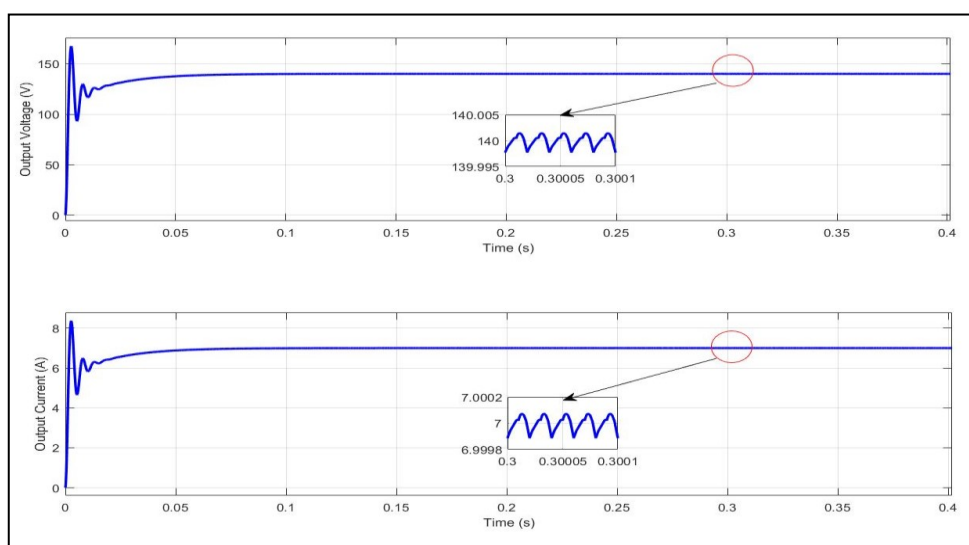


Figure 12. Output voltage and current for MIIBC with RE sources case II

From the simulation results of both conditions obtained as in Table 6. From the table, the values of the input current ripples for each case are quite high where these values are ± 0.1 A. However, these values are acceptable since their ripples current percentage are below than the set ripple percentage which is 20%. Also, based on the simulation results, it can be concluded that each condition case is able to reach the desired output voltage which is 140 V but depending on their own time. Where the higher duty cycle switches 2 (D_2), the less time is needed to reach desired output voltage.

Nevertheless, the output ripples of the converter show the expected result when the converter is using the interleaved method where low output ripples is produced. Output voltage and current waveforms have a lower ripple percentage which is good for the application system stability. Last but not least, the efficiency of the converter for each case in both conditions is obtained by using equation 14. From Table 6, the efficiency of each case is considered high which is more than 97%. This has proved that the designed converter is able to produce great system efficiency.

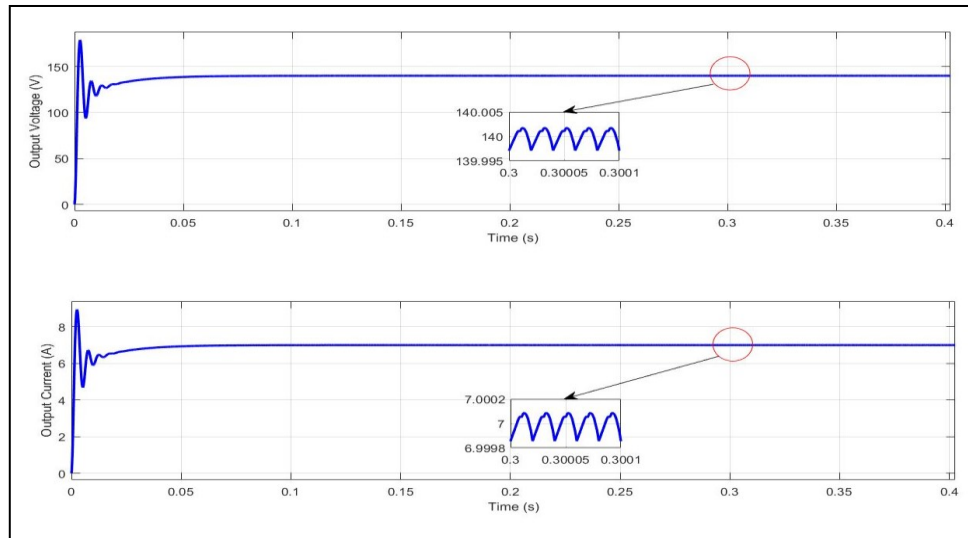


Figure 13. Output voltage and current for MIIBC with RE sources case III

Table 6. Comparison between each cases

Cases	I	II	III
Input current, I_s (A)	14.325	14.36	14.37
Input current ripple percentage (%)	0.523	0.905	1.044
Input current ripple, ΔI_s (A)	0.075	0.13	0.15
Time to reach desired output voltage (s)	0.09	0.055	0.045
Output Voltage ripple, ΔV_o (mV)	2.5	4.0	5.0
Output Current ripple, ΔI_o (mA)	0.13	0.15	0.2
Efficiency, η (%)	97.731	97.493	97.425

4. CONCLUSION

A multi-input interleaved boost converter has been proposed and verified in this study. Systematic modes of operation are discussed for double input two-phase interleaved boost converter which presented a different segment of the duty cycle of MOSFETs and IGBTs. Mathematical equations have been developed to a better understanding of the converter in terms of its operation and current sharing between two-phase inductors. A deep understanding of two types of renewable energy has also been considered where the renewable energy is solar PV array and PEMFC. Evidently, the increase of inductor current sharing leads to reducing ripples in input current. These ripples reduction leads to minimizing sizes of capacitor which also improves the overall proposed converter performance and lead to lower cost of system design. Future work will consist of investigating control techniques for renewable energy used and power losses study in multi-input interleaved boost converter and how to optimize the losses.





REFERENCES

- [1] S. Hazra, S. Madhusoodhanan, S. Bhattacharya, G. K. Moghaddam and K. Hatua, "Design considerations and performance evaluation of 1200 V, 100 a SiC MOSFET based converter for high power density application," *2013 IEEE Energy Conversion Congress and Exposition*, 2013, pp. 4278-4285, doi: 10.1109/ECCE.2013.6647272.
- [2] C. Chang, C. Cheng and H. Cheng, "Modeling and Design of the LLC Resonant Converter Used as a Solar-Array Simulator," in *IEEE Journal of Emerging and Selected Topics in Power Electronics*, vol. 2, no. 4, pp. 833-841, Dec. 2014, doi: 10.1109/JESTPE.2014.2349980.
- [3] M. Yilmaz, "Passive full-wave MOSFET rectifiers for electromagnetic harvesting," Dept. of Electrical and Computer Engineering, M.S. thesis, University of Waterloo, Waterloo, Ontario, Canada, 2013. Available: <http://hdl.handle.net/10012/7722>.
- [4] M. ElMenshawy and A. Massoud, "Multimodule DC-DC Converters for High-Voltage High-Power Renewable Energy Sources," *2019 2nd International Conference on Smart Grid and Renewable Energy (SGRE)*, 2019, pp. 1-6, doi: 10.1109/SGRE46976.2019.9020690.
- [5] A. Gopiyani and V. Patel, "A closed-loop control of high power LLC Resonant Converter for DC-DC applications," *2011 Nirma University International Conference on Engineering*, 2011, pp. 1-6, doi: 10.1109/NUIConE.2011.6153284.
- [6] C. Chen, X. Zhao and J. Lai, "A PWM Controlled Active Boost Quadrupler Resonant Converter for High Step-Up Application," *2019 IEEE Applied Power Electronics Conference and Exposition (APEC)*, 2019, pp. 2317-2321, doi: 10.1109/APEC.2019.8721831.
- [7] H. Cha, F. Z. Peng and D. Yoo, "Z-source resonant DC-DC converter for wide input voltage and load variation," *The 2010 International Power Electronics Conference - ECCE ASIA -*, 2010, pp. 995-1000, doi: 10.1109/IPEC.2010.5542140.
- [8] K. Varesi, S. H. Hosseini, M. Sabahi, E. Babaei, and N. Vosoughi, "Performance and design analysis of an improved non-isolated multiple input buck DC-DC converter," *IET Power Electronics*, vol. 10, no. 9, pp. 1034-1045, 2017, doi: 10.1049/iet-pel.2016.0750.
- [9] B. Ismail, M. M. Naain, N. I. A. Wahab, L. J. Awalin, I. Alhamrouni and M. F. A. Rahim, "Optimal placement of DSTATCOM in distribution network based on load flow and voltage stability indices studies," *2017 International Conference on Engineering Technology and Technopreneurship (ICE2T)*, 2017, pp. 1-6, doi: 10.1109/ICE2T.2017.8215973.
- [10] J. Cao and A. Emadi, "A New Battery/UltraCapacitor Hybrid Energy Storage System for Electric, Hybrid, and Plug-In Hybrid Electric Vehicles," *IEEE Transactions on Power Electronics*, vol. 27, no. 1, pp. 122-132, 2012, doi: 10.1109/TPEL.2011.2151206.
- [11] S. M. Tayebi, W. Xu, H. Wang, R. Yu, Z. Guo and A. Q. Huang, "A Single-Stage Isolated Resonant SiC DC/AC Inverter for Efficient High-Power Applications," *2020 IEEE Applied Power Electronics Conference and Exposition (APEC)*, 2020, pp. 399-404, doi: 10.1109/APEC39645.2020.9124343.
- [12] M. M. Ghahderijani, M. Castilla, A. Momeni, J. Miret, and L. G. de Vicuña, "Robust and fast sliding-mode control for a DC-DC current-source parallel-resonant converter," *IET Power Electronics*, vol. 11, no. 2, pp. 262-271, 2017, doi: 10.1049/iet-pel.2017.0033.
- [13] V. Wuti, A. Luangpol, K. Tattiwong, S. Trakuldit, A. Taylim and C. Bunlaksananusorn, "Analysis and Design of a Zero-Voltage-Switched (ZVS) Quasi-Resonant Buck Converter Operating in Full-Wave Mode," *2020 6th International Conference on Engineering, Applied Sciences and Technology (ICEAST)*, 2020, pp. 1-4, doi: 10.1109/ICEAST50382.2020.9165351.
- [14] I. Alhamrouni, M. B. Hamzah, M. Salem, A. Jusoh, A. B. Khairuddin, and T. Sutikno, "A bidirectional resonant converter based on wide input range and high efficiency for photovoltaic application," *International Journal of Power Electronics and Drive System (IJPEDS)*, vol. 10, pp. 1469-1475, 2019, doi: 10.11591/ijpeds.v10.i3.1469-1475.
- [15] E. H. E. Bayoumi, "Dual-input DC-DC converter for renewable energy," *Electromotion*, vol. 21, pp. 77-83, 2014.
- [16] I. Alhamrouni, A. B. Khairuddin, A. K. Ferdavani, M. Salem and A. Alnajja, "Differential evolution algorithm for multistage transmission expansion planning based on AC load flow model," *3rd IET International Conference on Clean Energy and Technology (CEAT)*, Kuching, Malaysia, 2014, pp. 1-4, doi: 10.1049/cp.2014.1468.
- [17] Y. M. Y. Buswigi, W. M. Utomo and Z. A. Haron, "Multi-Input Boost Converter for Hybrid PV and Wind Generator Systems," *Advanced Materials Research*, no. 925, pp. 619-624, 2014, doi: 10.4028/www.scientific.net/AMR.925.619.
- [18] I. Alhamrouni, W. Wahab, M. Salem, N. H. A. Rahman and Lili Awalin, "Modeling of Micro-grid with the consideration of total harmonic distortion analysis," *Indonesian Journal of Electrical Engineering and Computer Science (IJECS)*, vol. 15, pp. 581-592, 2019, doi: 10.11591/ijeecs.v15.i2.pp581-592.
- [19] M. C. Mira, Z. Zhang, A. Knott and M. A. E. Andersen, "Analysis, Design, Modeling, and Control of an Interleaved-Boost Full-Bridge Three-Port Converter for Hybrid Renewable Energy Systems," *IEEE Transactions on Power Electronics*, vol. 32, no. 2, pp. 1138-1155, 2017, doi: 10.1109/TPEL.2016.2549015.
- [20] N. Agrawal, S. Samanta and S. Ghosh, "Multiple-Input Interleaved Boost Converter for High Power Application," *IEEE International Conference on Power Electronics, Drives and Energy Systems (PEDES)*, 2018, pp. 1-5, doi: 10.1109/PEDES.2018.8707770.
- [21] I. Alhamrouni, M. A. Alif, B. Ismail, M. Salem, A. Jusoh, and T. Sutikno, "Load flow based voltage stability indices for voltage stability and contingency analysis for optimal location of STATCOM in distribution network with integrated distributed generation unit," *Telecommunication, Computing, Electronics and Control TELKOMNIKA*, vol. 16, no. 5, pp. 2302-2315, 2018, doi: 10.12928/TELKOMNIKA.v16i5.10577.
- [22] S. Abolhosseini, A. Heshmati and J. Altmann, "A Review of Renewable Energy Supply and Energy Efficiency Technologies," *IZA Discussion Paper*, pp. 1-36, 2014, doi: 10.2139/ssrn.2432429.
- [23] Texas Instrument, "Phase Shifted, Zero Voltage Transition Design Configuration," *Application Report*, pp. 1-19, 2011.
- [24] N. Smith and R. McCann, "Analysis and simulation of a multiple input interleaved boost converter for renewable energy applications," *2014 IEEE 36th International Telecommunications Energy Conference (INTELEC)*, 2014, pp. 1-7, doi: 10.1109/INTLEC.2014.6972129.
- [25] U. Kundu, K. Yenduri and P. Sensarma, "Accurate ZVS Analysis for Magnetic Design and Efficiency Improvement of Full-Bridge LLC Resonant Converter," in *IEEE Transactions on Power Electronics*, vol. 32, no. 3, pp. 1703-1706, March 2017, doi: 10.1109/TPEL.2016.2604118.
- [26] S. A. Gorji, M. Ektesabi and J. Zheng, "Double-input boost/Y-source DC-DC converter for renewable energy sources," *2016 IEEE 2nd Annual Southern Power Electronics Conference (SPEC)*, 2016, pp. 1-6, doi: 10.1109/SPEC.2016.7846020.
- [27] I. Alhamrouni, M. Iskander, M. Salem, L. Awalin, A. Jusoh, and T. Sutikno, "Application of inductive coupling for wireless power transfer," *International Journal of Power Electronics and Drive Systems*, vol. 11, no. 3, pp. 1109-1116, Sep. 2020, doi: 10.11591/ijpeds.v11.i3.pp1109-1116.





- [28] F. Canales, P. Barbosa and F. C. Lee, "A wide input voltage and load output variations fixed-frequency ZVS DC/DC LLC resonant converter for high-power applications," *Conference Record of the 2002 IEEE Industry Applications Conference. 37th IAS Annual Meeting (Cat. No.02CH37344)*, 2002, pp. 2306-2313 vol.4, doi: 10.1109/IAS.2002.1042768.
- [29] X. Wang, G. Tang, Z. He, X. Wei, H. Pang and X. Xiao, "Modeling and control of an isolated module multilevel DC/DC converter for DC grid," in *CSEE Journal of Power and Energy Systems*, vol. 3, no. 2, pp. 150-159, June 2017, doi: 10.17775/CSEEJPES.2017.0019.
- [30] World Energy Council, "World Energy Resources 2016," 2016. Available: <https://www.worldenergy.org/assets/images/imported/2016/10/World-Energy-Resources-Full-report-2016.10.03.pdf>
- [31] K. P. Rao, S. Sao, J. B. V. Subrahmanyam, "Design and Analysis of a Novel Multilevel Inverter Topology Suitable for Renewable Energy Sources Interfacing to AC Grid for High Power Application," *International Journal of Scientific and Research Publications*, vol. 3, no. 5, May 2013.
- [32] B. R. Lin, and W. J. Lin, "Half-bridge zero voltage switching converter with three resonant tanks," *Journal of Power Electronics*, vol. 14, no. 5, pp. 882–889, 2014, doi: 10.6113/JPE.2014.14.5.882.
- [33] H. Wu, Y. Lu, T. Mu and Y. Xing, "A Family of Soft-Switching DC–DC Converters Based on a Phase-Shift-Controlled Active Boost Rectifier," in *IEEE Transactions on Power Electronics*, vol. 30, no. 2, pp. 657-667, Feb. 2015, doi: 10.1109/TPEL.2014.2308278.
- [34] R. Chowdhury and T. Boruah, "Design of a Micro-Grid System in Matlab/Simulink," *International Journal of Innovative Research in Science, Engineering and Technology*, vol. 4, no. 7, July 2015, doi: 10.15680/IJRSET.2015.0407030.
- [35] G. Chen, X. Li and S. Zhou, "Unified Boundary Control With Phase Shift Compensation for Dual Bridge Series Resonant DC-DC Converter," in *IEEE Access*, vol. 8, pp. 131137-131149, 2020, doi: 10.1109/ACCESS.2020.3010007.
- [36] A. N. Rahman, C. Lee, H. Chiu and Y. Hsieh, "Bidirectional Three-Phase LLC Resonant Converter," *2018 IEEE Transportation Electrification Conference and Expo, Asia-Pacific (ITEC Asia-Pacific)*, 2018, pp. 1-5, doi: 10.1109/ITEC-AP.2018.8433271.

BIOGRAPHIES OF AUTHORS







Ibrahim Alhamrouni     received his B.Eng. degree in electrical engineering from Elmergib University, Al Khums, Libya, in 2008. The M.Sc. degree in electrical power engineering from Universiti Tun Hussein Onn Malaysia (UTHM), Batu Pahat, Johor, Malaysia, in 2011. In 2015, he has been awarded his Ph.D degree from Faculty of Electrical Engineering, Universiti Teknologi Malaysia (UTM), Malaysia. Currently, he is a senior lecturer and researcher at the British Malaysian Institute, University of Kuala Lumpur, Malaysia. His research interest includes Power System Planning and Operation, Deregulation and Restructuring of Power System and power lines maintenance. He's currently working on Micro-grid technologies and the Application of Power Electronics in Power System. He can be contacted at: ibrahim.mohamed@unikl.edu.my







Mohamed Salem     received the B.Eng.in electrical and power engineering from Elmergib University, Libya, in 2008. The M.Sc. of electrical engineering from (UTHM), Malaysia, in 2011. In August 2017, he has been awarded his Ph.D degree from Department of Power Engineering, Faculty of Electrical Engineering, Universiti Teknologi Malaysia. He is a member of IEEE, and a registered graduate engineers Malaysia (BEM) in the electrical track. Currently, he is a senior lecturer at School of Electrical and Electronic Engineering, Universiti Sains Malaysia, Penang, Malaysia since July 2018. He has authored and co-authored number of well recognized journals and conference papers. His research interests are in DC-DC converter, renewable energy applications, and control of power electronic systems. He can be contacted at: salemm@usm.my.







Zahraoui Younes     received the B.S. and M.S. degrees from Hydrocarbons and Chemistry at the University M'hamed Bougara, Boumerdes, Algeria, in 2015 and 2017, respectively. He is currently pursuing a Ph.D. degree with Kuala Lumpur University, Malaysia. He is with the campus of Electronic Information and Electrical Engineering, British Malaysian Institute. His current research interests include power system optimization, renewable energy and evolutionary algorithms. He can be contacted at email: zahraoui.younes@s.unikl.edu.my.







Bazilah Ismail     received the BEng in electrical & electronics from the University of Sheffield, UK in 2011, the M.Sc. degree in Sustainable electrical power engineering from Brunel University London, UK, in 2014. Currently, she is a lecturer at the electrical engineering section, British Malaysian Institute, Universiti Kuala Lumpur. Her research interest includes FACTS device and smart grid applications for voltage system stability improvement. She can be contacted on the email: bazilahismail@unikl.edu.my



Awang Jusoh     was born in Terengganu, Malaysia in 1964. He received his B.Eng. degree from Brighton Poly-technic, U.K., in 1988. He obtained his M.Sc. and Ph.D. degrees from the University of Birmingham, U.K., in 1995 and 2004, respectively. He is currently an associated Professor in the Department of Power Engineering, Faculty of Electrical Engineering, Universiti Teknologi Malaysia UTM, Johor, Malaysia. His research interests are in DC-DC converter, renewable energy, and control of power electronics systems. He can be contacted on the email: awang@fke.utm.my.



Tole Sutikno     is a Lecturer in Electrical Engineering Department at the Universitas Ahmad Dahlan (UAD), Yogyakarta, Indonesia. He received his B.Eng., M.Eng. and Ph.D. degrees in Electrical Engineering from Universitas Diponegoro, Universitas Gadjah Mada and Universiti Teknologi Malaysia, in 1999, 2004 and 2016, respectively. He has been an Associate Professor in UAD, Yogyakarta, Indonesia since 2008. He is currently an Editor-in-Chief of the TELKOMNIKA since 2005, and the Head of the Embedded Systems and Power Electronics Research Group since 2016. His research interests include the field of industrial applications, industrial electronics, industrial informatics, power electronics, motor drives, renewable energy, FPGA applications, embedded system, image processing, artificial intelligence, intelligent control, digital design and digital library. He can be contacted on the email: tole@ee.uad.ac.id.